

1. Report No. FHWA/TX-04/0-2135-1		2. Government Accession No.		3. Recipient's Catalog No.	
4. Title and Subtitle Optimal Inspection of Fracture-Critical Steel Trapezoidal Girders				5. Report Date October 2003	
				6. Performing Organization Code	
7. Author(s) Hsin-Yang Chung, Lance Manuel, and Karl H. Frank				8. Performing Organization Report No. Research Report 0-2135-1	
9. Performing Organization Name and Address Center for Transportation Research The University of Texas at Austin 3208 Red River, Suite 200 Austin, TX 78705-2650				10. Work Unit No. (TRAIS)	
				11. Contract or Grant No. Research Project 0-2135	
12. Sponsoring Agency Name and Address Texas Department of Transportation Research and Technology Implementation Office P.O. Box 5080 Austin, TX 78763-5080				13. Type of Report and Period Covered Research Report	
				14. Sponsoring Agency Code	
15. Supplementary Notes  Project conducted in cooperation with the U.S. Department of Transportation, Federal Highway Administration, and the Texas Department of Transportation.					
16. Abstract  A reliability-based procedure for inspection scheduling of steel bridges is proposed to yield the optimal (most economical) inspection strategy that meets an acceptable safety level through the planned service life. Two fatigue reliability formulations that can be applied for most details in steel bridges are presented. For details classified according to AASHTO fatigue categories, a limit state function related to the number of stress cycles to failure based on Miner's rule is used to evaluate the fatigue reliability; for details not classified according to AASHTO fatigue categories, a limit state function related to crack size and growth rate is used to evaluate the fatigue reliability. The inspection scheduling problem is modeled as an optimization problem with an objective function that includes the total expected cost of inspection, repair, and failure formulated using an event tree approach, appropriate constraints on the interval between inspections, and a specified minimally acceptable (target) structural reliability. An optimal inspection-scheduling plan can thus be developed for any specified fatigue details or fracture-critical sections in steel bridges. Examples presented demonstrate the advantage of the reliability-based optimal inspection scheduling in cost saving and structural reliability control over alternative inspection plans.					
17. Key Words reliability, optimization, fracture-critical inspections, fatigue			18. Distribution Statement No restrictions. This document is available to the public through the National Technical Information Service, Springfield, Virginia 22161.		
19. Security Classif. (of report) Unclassified		20. Security Classif. (of this page) Unclassified		21. No. of pages 32	22. Price



**OPTIMAL INSPECTION OF FRACTURE-CRITICAL STEEL  
TRAPEZOIDAL GIRDERS**

*by*

**Hsin-Yang Chung, Lance Manuel, and Karl H. Frank**

Report 0-2135-1

Research Project 0-2135

GUIDELINES FOR INSPECTION OF FRACTURE CRITICAL STEEL TRAPEZOIDAL GIRDERS

Conducted for the

**TEXAS DEPARTMENT OF TRANSPORTATION**

in cooperation with the

**U.S. DEPARTMENT OF TRANSPORTATION**

**Federal Highway Administration**

by the

**CENTER FOR TRANSPORTATION RESEARCH**

Bureau of Engineering Research

**THE UNIVERSITY OF TEXAS AT AUSTIN**

October 2003

## **DISCLAIMERS**

The contents of this report reflect the views of the authors, who are responsible for the facts and the accuracy of the data presented herein. The contents do not necessarily reflect the official views or policies of the Federal Highway Administration or the Texas Department of Transportation. This report does not constitute a standard, specification, or regulation.

There was no invention or discovery conceived or first actually reduced to practice in the course of or under this contract, including any art, method, process, machine, manufacture, design or composition of matter, or any new and useful improvement thereof, or any variety of plant, which is or may be patentable under the patent laws of the United States of America or any foreign country.

**NOT INTENDED FOR CONSTRUCTION,  
BIDDING, OR PERMIT PURPOSES**

Lance Manuel  
Karl H. Frank, P.E. (Texas No. 48953)  
*Research Supervisors*

## **ACKNOWLEDGMENTS**

The authors gratefully acknowledge the financial support through a research grant awarded by the Texas Department of Transportation as part of the project, Inspection Guidelines for Fracture Critical Steel Trapezoidal Girders, directed by Mr. Alan Kowalik.

***Research performed in cooperation with the Texas Department of Transportation  
and the U.S. Department of Transportation, Federal Highway Administration.***

## TABLE OF CONTENTS

CHAPTER 1. INTRODUCTION.....	1
1.1 Background.....	1
1.2 Organization of the Report.....	1
CHAPTER 2. STRESS RANGE ANALYSIS OF FATIGUE LOADINGS IN STEEL BRIDGES .....	3
2.1 Background.....	3
2.2 Stress Spectrum Analysis.....	3
2.3 Rayleigh Distribution Analysis.....	3
2.4 Fatigue Truck Analysis.....	4
CHAPTER 3. FATIGUE RELIABILITY ANALYSIS FOR FRACTURE-CRITICAL MEMBERS.....	5
3.1 Objectives.....	5
3.2 Target Reliability Index.....	5
3.3 Fatigue Reliability Analysis for Details Classified in AASHTO Categories.....	5
3.4 Fatigue Reliability Analysis for Details Not Classified in AASHTO Categories.....	7
CHAPTER 4. OPTIMAL INSPECTION SCHEDULING .....	9
4.1 Background.....	9
4.2 Event Tree Analysis.....	9
4.3 Likelihood of Needed Repair.....	10
4.4 Cost of Inspections.....	11
4.5 Cost of Repairs.....	11
4.6 Cost of Failure.....	11
4.7 Total Cost.....	12
4.8 Constraints.....	12
4.9 Formulation of the Optimization Problem.....	13
CHAPTER 5. NUMERICAL EXAMPLES .....	15
5.1 Plate Girder Bridge Example.....	15
5.2 Box Girder Bridge Example.....	16
5.3 General Conclusions.....	16
CHAPTER 6. DISCUSSION AND CONCLUSIONS.....	25
REFERENCES.....	27



# CHAPTER 1. INTRODUCTION

## 1.1 BACKGROUND

To prevent members in steel bridges from fatigue failure, one usually needs to perform frequent periodic bridge inspections and employ detailed inspection methods. This is especially true for fracture-critical members or details. Carrying out these inspections puts a large burden on a transportation agency's bridge maintenance budget. A systematic reliability-based method for inspection scheduling is proposed to yield the most economical inspection strategy for steel bridges that, at the same time, guarantees an acceptable safety level through the planned service life. The inspection scheduling problem is modeled as an optimization problem with a well-defined objective function, that includes the total expected cost of inspection, repair and failure formulated on the basis of an event tree framework, and appropriate constraints in inspection intervals and minimum (target) structural reliability. An optimal inspection-scheduling plan can thus be obtained for any specified fatigue details (fracture-critical details) in steel bridges. Examples presented demonstrate the advantage of the reliability-based optimal inspection scheduling in cost saving and structural reliability control over alternative periodic inspection plans.

A reliability-based inspection scheduling procedure that can yield an optimal inspection schedule and can maintain a specified safety level for fracture-critical members in steel bridges through their planned service lives is presented. This procedure is based, in sequence, on a stress range analysis, a fatigue reliability analysis, and an optimization analysis. In the stress range analysis, the "effective" stress range for the identified member or detail may be obtained from a stress spectrum analysis, an assumed stress probability distribution (e.g., Rayleigh) based on data, or a fatigue truck analysis. Once this effective stress range distribution representative of the actual traffic on a bridge is obtained, a fatigue reliability analysis of the member or detail of interest may be performed. For all details classified in specific AASHTO fatigue categories, a limit state function related to the number of stress cycles to failure that is based on Miner's Rule may be used; for all other details (i.e., not classified in specific AASHTO fatigue categories), a limit state function based on crack growth rates, as proposed by Madsen (1985), may be used. An optimization problem for inspection scheduling that incorporates fatigue reliability calculations (for details of interest) along with an event tree approach, is formulated with an objective function includes costs and appropriate constraints on the inspection intervals and on acceptable minimum levels of structural safety. Solution of the optimization problem yields the optimal inspection schedule. Numerical examples from two case studies on steel bridges – one including a plate girder, the other including a box girder – are presented to demonstrate the proposed reliability-based optimal inspection scheduling procedure.

## 1.2 ORGANIZATION OF THE REPORT

Chapter 2 of this report provides a description of the various approaches that may be followed in the stress range analysis studies needed for any fatigue assessment of a steel bridge member or detail. Chapter 3 covers topics related to the fatigue reliability analysis for details classified according to AASHTO category as well as for those that are not. Chapter 4 presents the formulation of the optimization problem for inspection scheduling. Chapter 5 includes numerical examples that contain optimum inspection schedules for two details on two different bridges. Chapter 6 includes some general conclusions and discussions related to this research study.





## CHAPTER 2. STRESS RANGE ANALYSIS OF FATIGUE LOADINGS IN STEEL BRIDGES

### 2.1 BACKGROUND

The operating stress range for steel members or details in bridges is a key factor that directly affects the fatigue performance of members or details in steel bridges. Therefore, obtaining an accurate description of the effective stress range,  $S_{RE}$ , applied on the identified detail is very important in fatigue reliability analysis. Generally, any one of three methods: a stress spectrum analysis, a Rayleigh distribution analysis; or a fatigue truck analysis, may be applied to establish the effective stress range.

### 2.2 STRESS SPECTRUM ANALYSIS

If stress range data on a desired detail are systematically collected and sufficiently representative of actual traffic loads, a stress range spectrum can be derived from such data. For variable-amplitude stress ranges on details, Schilling et al. (1978) proposed an effective stress range  $S_{RE}$  to characterize a stress range spectrum and this value can be applied in Miner's Rule (see Miner, 1945) for fatigue analysis. This effective stress range  $S_{RE}$  is defined as the root mean cube (RMC) of the collected stress range data:

$$S_{RE} = \left\{ \sum_{i=1}^n \gamma_i \cdot S_{R,i}^3 \right\}^{1/3} \quad (1)$$

where  $\gamma_i$  is the ratio of the number of  $S_{R,i}$  stress range amplitude cycles to the total number of cycles. Schilling (1978) concluded that this definition of an effective stress range satisfactorily relates variable- and constant- amplitude results. Effective stress ranges,  $S_{RE}$  derived thus from a representative stress spectrum of a desired detail can be very accurate descriptions of the stresses for fatigue analysis of the detail. However, collecting stress data using strain gages is costly as well as difficult or restrictive for complex details. Another way to circumvent this problem is to convert the stress data collected from one detail to other uninstrumented details but this conversion can lead to large errors. Hence, this stress spectrum analysis approach is suitable only for those details monitored by strain gages that can yield the necessary stress spectrum.

### 2.3 RAYLEIGH DISTRIBUTION ANALYSIS

On the basis of the analysis of 51 sets of stress range spectrum data on bridges from 6 sources including Interstate and U.S. routes in semi-rural and metropolitan locations, Schilling et al. (1978) showed that a Rayleigh distribution can provide a reasonable model for the stress range spectrum of details in steel bridges. The Rayleigh probability density function for the stress range,  $S_R$ , can be expressed as:

$$f_{S_{RE}}(s_{RE}) = \left( \frac{s_{RE}}{S_{R0}^2} \right) \cdot \exp \left[ -\frac{1}{2} \left( \frac{s_{RE}}{S_{R0}} \right)^2 \right]; \quad \text{where } S_{R0} = \sqrt{\frac{2}{\pi}} E(S_{RE}) \quad (2)$$

The mean stress range effect of  $(S_R)^B$  can then be computed in closed form and applied in a Miner's rule format as follows:

$$E[S_R^B] = \sum_{i=1}^n \gamma_i \cdot S_{R,i}^B = (\sqrt{2}S_{R0})^B \cdot \Gamma\left(\frac{B}{2} + 1\right) = S_{RE}^B \quad (3)$$

## 2.4 FATIGUE TRUCK ANALYSIS

Another convenient way to evaluate  $S_{RE}$  for a desired detail is to apply an “effective” fatigue truck (representative in a fatigue sense of all the actual trucks on the bridge) in a structural analysis to obtain an effective stress range  $S_{RE}$ . According to the Weight-In-Motion (WIM) data research from FHWA in 1981 (see Snyder et al, 1985), an HS15 (weight = 54 kips) fatigue truck was proposed and has been adopted in the AASHTO Specifications (1998). Due to the different volume and characteristics of current traffic from that of the 1980s, this definition of an HS15 fatigue truck suggested in the AASHTO Specifications needs to be re-examined. Weight-In-Motion (WIM) data collected directly from the traffic site, especially without the knowledge of drivers, can help to establish an improved definition of the effective fatigue truck. The effective gross vehicle weight,  $GVW_E$ , calculated from the RMC of the load spectrum from WIM data can be taken as the weight of the fatigue truck.

$$GVW_E = \left\{ \sum_{i=1}^n \alpha_i \cdot GVW_i^3 \right\}^{1/3} \quad (4)$$

where  $\alpha_i$  is the relative likelihood of trucks with gross vehicle weight,  $GVW_i$  in the overall truck load spectrum. One can take this value of  $GVW_E$  as the weight of a new fatigue truck and then distribute this weight to the fatigue truck in a similar manner as is done with the HS15 effective fatigue truck in the AASHTO Specifications. A more detailed study on axle spacings can help and is a topic of ongoing study. With such information, one could apply WIM data to simulate actual truck passages along a bridge. The moment range,  $M_R$ , resulting from each truck can be obtained from a moment influence line analysis using standard structural analysis programs. An effective moment range,  $M_{RE}$ , can then be computed:

$$M_{RE} = \left\{ \sum_{i=1}^n \alpha_i \cdot M_{R,i}^3 \right\}^{1/3} \quad (5)$$

where  $M_{R,i}$  is the moment range resulting from the truck with weight,  $GVW_i$ . The effective of fatigue truck configuration in terms of axle spacings and weights, then, is that which results in the moment range,  $M_{RE}$ , on the same bridge and where the total axle weights equal  $GVW_E$ . Suitable axle spacings and axle weights for the fatigue truck can then be derived. After applying an effective fatigue truck as a live load on the bridge with an appropriate impact factor ( $I$ ) and a distribution factor ( $DF$ ), an influence line analysis may be performed and the effective stress range,  $S_{RE}$ , can be obtained (see Schilling, 1982a, b).

## CHAPTER 3. FATIGUE RELIABILITY ANALYSIS FOR FRACTURE-CRITICAL MEMBERS

### 3.1 OBJECTIVES

Our objective here is to apply reliability theory to evaluate the safety of fracture-critical members (details) under fatigue loadings in their service lives. The AASHTO fatigue analysis approach is presented for details classified according to AASHTO fatigue categories. After defining a target reliability, a minimum acceptable level for structural safety, the actual reliability for the chosen fracture-critical detail may be compared with this target to provide information for subsequent inspection schedules.

### 3.2 TARGET RELIABILITY INDEX

The target reliability index,  $\beta_{min}$ , is defined as the minimum safety level approved and accepted by all or most of the individuals in a specific application. In our problem, this value can be applied as a standard, against which one can measure the safety of the identified detail or member. The target reliability index,  $\beta_{min}$ , can be given in terms of the inverse of the cumulative distribution function of a standard Gaussian random variable,  $\Phi$ , and a maximum acceptable probability of failure,  $P_F$ :

$$\beta_{min} = \Phi^{-1}(1 - P_F) \quad (6)$$

### 3.3 FATIGUE RELIABILITY ANALYSIS FOR DETAILS CLASSIFIED IN AASHTO CATEGORIES

In the AASHTO Specifications, empirical S-N curve relations were established from fatigue tests conducted in the 1970s to prevent design details in steel bridges from fatigue failure. Eight categories, designated as A to E' in the specifications, are tabulated to classify details in steel bridges and to provide information for the S-N curve relation that can be expressed as:

$$N = A \cdot S_R^{-3} \quad (7)$$

where  $N$  is the number of constant-amplitude stress cycles of range,  $S_R$ , applied on the specified detail that cause failure, and  $A$  is a parameter that can be obtained from fatigue tests (each fatigue category has a different value of  $A$ ). Thus, for any detail, one can obtain either the expected fatigue life  $N$  in terms of number of stress cycles under a design stress range, or a limit stress range for desired service life.

Because of randomness in the actual traffic loadings, stress ranges are not of constant amplitude. Therefore, Miner (1945) proposed an empirical rule to evaluate the fatigue damage,  $D$ , under variable-amplitude stress ranges as follows:

$$D = \sum \frac{n_i}{N_i} \geq \Delta \quad (8)$$

where  $D$  is Miner's damage accumulation index,  $n_i$  is the actual number of cycles with constant stress range amplitude,  $S_{R,i}$ , and  $N_i$  is the number of cycles that the detail can sustain under the same constant stress range,  $S_{R,i}$ . Fatigue damage of the specified detail occurs when  $D$  exceeds  $\Delta$ . The

parameter,  $\Delta$ , is around 1.0 for metallic materials based on Miner's observations. Combining the S-N curve relation with Miner's rule, we have:

$$D = \sum \frac{n_i}{N_i} = \sum \frac{\gamma_i \cdot N}{A \cdot S_{R,i}^{-3}} = \frac{N}{A} \sum [\gamma_i \cdot S_{R,i}^3] = \frac{N}{A} S_{RE}^3 \geq \Delta \quad (9)$$

where  $N$  is the total number of stress cycles at all stress levels,  $\square_i$  is the ratio of  $n_i$  to  $N$ , and  $S_{RE}$  is the effective stress range calculated, for example, from the RMC (root mean cube) of the stress spectrum for the specified detail.

When  $D$  equals  $\Delta$  in Eq. (9), the critical number of stress cycles  $N_c$  to fatigue failure under the variable-amplitude loading with effective stress range,  $S_{RE}$ , can be represented as:

$$N_c = \frac{A \cdot \Delta}{S_{RE}^3} \quad (10)$$

The fatigue property,  $A$ , of a specific detail may be modeled as a lognormal random variable based on the statistical stress range data derived by Moses et al. (1987) from the test results reported by Keating and Fisher (1985). It is assumed here that for each of five fatigue categories (A to E),  $A$  followed a lognormal distribution with a mean value,  $\mu$ , and coefficient of variation, COV or  $\delta$ , as shown in Table 1. In addition, Wirsching and Chen (1988) studied the test data reported by Miner (1945) and found that  $\Delta$  may also be modeled by a lognormal distribution with a mean value of 1.0 and a COV of 0.30. Since  $A$  and  $\square$  are random variables, according to Eq. (10),  $N_c$  is also a random variable. Similar to the treatment by Zhao et al. (1994), we propose a limit state function  $g(\mathbf{X})$  for fatigue reliability analysis, which is defined in terms of  $N_c$  (the number of cycles to failure for the detail) and  $N$  (the actual number of cycles to which the detail is subjected):

$$g(\mathbf{X}) = N_c - N = \frac{A \cdot \Delta}{S_{RE}^3} - N \quad (11)$$

where  $g(\mathbf{X}) < 0$  implies failure. The number of stress cycles,  $N$ , is computed from truck passages. With knowledge of the number of stress cycles per truck passage ( $C_s$ ) and the Average Daily Truck Traffic (ADTT), the number of stress cycles,  $N$ , can be related to the number of years of operation,  $Y$ :

$$N(Y) = 365 \times C_s \times \text{ADTT} \times Y \quad (12)$$

The fatigue failure event of a detail can then be defined as

$$g(\mathbf{X}) = N_c - N(Y) \leq 0 \quad (13)$$

The probability of fatigue failure for the detail in question can then be related to a reliability index,  $\beta$ , and evaluated as:

$$P_f = P(g(\mathbf{X}) \leq 0) = \Phi(-\beta) \quad (14)$$

If the random variables  $A$  and  $\Delta$  are assumed to follow lognormal distributions, the reliability index  $\beta$  can be directly expressed as:

$$\beta = \frac{(\lambda_\Delta + \lambda_A) - 3 \ln S_{RE} - \ln(N)}{\sqrt{\zeta_\Delta^2 + \zeta_A^2}} \quad (15)$$

where the parameters,  $\lambda_{\Delta}$ ,  $\lambda_A$ ,  $\zeta_{\Delta}$ , and  $\zeta_A$  are given in terms of the mean ( $\mu$ ) and the coefficient of variation ( $\delta$ ) of  $A$  and  $\Delta$  as follows:

$$\lambda_A = \ln(\mu_A) - \frac{\zeta_A^2}{2}, \lambda_{\Delta} = \ln(\mu_{\Delta}) - \frac{\zeta_{\Delta}^2}{2}; \quad \zeta_A = \sqrt{\ln(1 + \delta_A^2)}, \zeta_{\Delta} = \sqrt{\ln(1 + \delta_{\Delta}^2)} \quad (16)$$

Note that  $S_{RE}$  in Eq. (15) can be evaluated from a stress spectrum analysis, a Rayleigh distribution analysis, or a fatigue truck analysis as described earlier. This AASHTO reliability analysis approach can be applied to any detail classified by AASHTO fatigue category.

### 3.4 FATIGUE RELIABILITY ANALYSIS FOR DETAILS NOT CLASSIFIED IN AASHTO CATEGORIES

To analyze the fatigue reliability of details that are not categorized in the AASHTO fatigue categories, a fatigue limit state function,  $g(\mathbf{X})$ , related to crack size, as proposed by Madsen (1985), is applied. This limit state function,  $g(\mathbf{X})$ , is expressed as:

$$g(\mathbf{X}) = \psi(a_c) - \psi(a_N) \leq 0 \quad (17a)$$

$$\psi(a_c) = \int_{a_0}^{a_c} \frac{da}{(Y(a)\sqrt{\pi a})^B} \quad (17b)$$

$$\psi(a_N) = C \cdot S_{RE}^B \cdot N \quad (17c)$$

where  $a_c$  = the critical crack size associated with failure;  $a_N$  = the crack size corresponding to  $N$  stress cycles;  $a_0$  = initial crack size;  $\psi(a)$  = a damage accumulation function resulting from change in crack size from  $a_0$  to  $a$ ;  $C$  = a material property;  $B$  = an equivalent-damage material property consistent with Eq. (3);  $Y(a)$  = a geometry function accounting for the shape of the specimen and mode of fracture.

As before, the probability of failure and associated reliability index may be evaluated using Eq. (14). Solution for  $P_F$  or  $\beta$  may be obtained by FORM, SORM, or Monte Carlo simulation once all the random variables and their distributions are defined.

**TABLE 1 Mean and Coefficient of Variation (COV) of the Fatigue Parameter,  $A$ .**

AASHTO Category	$\mu_A$ (Mean Value)	$\delta_A$ COV
A	$1.50 \times 10^{11}$	0.54
B	$7.85 \times 10^{10}$	0.35
C	$1.10 \times 10^{10}$	0.15
D	$4.76 \times 10^9$	0.25
E	$2.01 \times 10^9$	0.26



## CHAPTER 4. OPTIMAL INSPECTION SCHEDULING

### 4.1 BACKGROUND

Currently, scheduling of inspections to prevent steel bridges from fatigue failure is based on a two-year periodic pattern required by the Federal Highway Administration (FHWA) and the responsible engineer's experience. However, every steel bridge has its own specific geometric shape, design philosophy, and traffic condition, and even on a single bridge, details may be classified into any of eight fatigue categories and might experience quite different levels of stress ranges. The different fatigue category and the stress range can result in different fatigue lives for each detail. Hence, a specific fixed inspection interval schedule may not meet the inspection demands of all types of fatigue details in a steel bridge. Besides, a periodic inspection schedule will lead to a fixed number of inspections over the service life of the bridge. This number of inspections may be more than the demands for some fatigue details and less for others. If the cost of an inspection is high, such as is the case for a FCM (Fracture-Critical Member) inspection which is usually expensive to perform and causes other traffic inconveniences, a greater number of inspection times will increase the budget burden for the transportation agency. Thus, the present strategy of inspection scheduling may be not only uneconomical but also inadequate from a safety point of view. A method of inspection scheduling for steel bridges based on reliability theory and optimization that can yield a balanced solution that takes into consideration both economical and safety aspects is proposed.

Reliability-based inspection scheduling has been applied in many areas of engineering. Thoft-Christensen and Sorensen (1987), Madsen (1989) and Sorensen et al. (1991) applied such reliability-based inspection strategies to offshore structures. Frangopol et al. (1997) utilized such inspection strategies for reinforced concrete bridges. For corrosion problems in steel girder bridges, Sommer et al. (1993) proposed a reliability-based strategy for inspection scheduling. The general approach in all such applications is to formulate the inspection scheduling problem as an optimization problem that seeks to minimize a cost function (the objective function) by adjusting inspection times within appropriate constraints and simultaneously maintaining safety constraints as well.

In our problem, let us first consider a single fatigue detail. The cost function for this detail is composed of the cost of inspections, repairs and structure failure during the service life. An event tree analysis that simulates all the possible scenarios after every inspection during the service life can be formulated. Fatigue reliability results obtained using the AASHTO approach are applied and transformed into appropriate probabilistic form for the event tree analysis.

### 4.2 EVENT TREE ANALYSIS

After every inspection of a fatigue detail, possible actions of "repair" and "no repair" are enumerated to construct the event tree for this detail over the service life. An example of an event tree, which is similar to one suggested by Frangopol et al. (1997), is shown in Fig. 1. From the year  $T_0$  when the detail is assumed to come into use till the year  $T_1^-$  when the first inspection is about to be performed, the detail is assumed not to have had any repair; so, a single horizontal branch can represent the status of the detail from  $T_0$  to  $T_1^-$ . The time spent during inspection is assumed to be negligibly short. After the first inspection at  $T_1^+$ , a repair decision has to be made according to the inspection results for the fatigue detail. If a crack is detected and the crack size is over the size limit defined to be that needing repair, a repair action is assumed to be implemented immediately. The time spent during repair is also assumed to be negligibly short in this study but this assumption can easily be relaxed. If no crack is detected or the crack size can be tolerated (i.e., it is smaller than a size that warrants

repair), no repair action should be taken. Hence, the original single horizontal branch modeling the fatigue detail's status at  $T_1$  is bifurcated into two branches; one branch models the detail status after repair from  $T_1^+$  to  $T_2^-$  (the time just preceding the second inspection) and the other branch models the status without any repair from  $T_1^+$  to  $T_2^-$  (in Fig. 1, a branch designated "1" represents a repair action and a branch designated "0" represents a no-repair action). Both branches are bifurcated again at  $T_2^+$  just after the second inspection is completed to model the repair status of the detail. Continuing onward, each branch in the event tree will be bifurcated again and again immediately after every inspection is completed until the service life,  $T_f$ , is reached. Therefore, the event tree simulates all the possible repair realizations in all of the branches during the planned service life. If  $n$  inspections are performed during the service life of a detail,  $2^n$  branches will be generated at the end of the event tree, implying that  $2^n$  possible scenarios will happen in the future. Note that in the optimization problem to be formulated, we will be attempting to determine the number  $n$  of inspections and the times of these inspections,  $T_1, T_2, \dots, T_n$ .

The fatigue reliability, modeled as a decreasing function,  $\beta(T)$ , obtained from the AASHTO fatigue analysis for the desired fatigue detail will be greatly affected by the repair realizations after each inspection. In this study, an assumption is made that the detail after repair will be as good as new. Thus, the fatigue reliability at every inspection time point will be raised (or updated) to the same level as that at the starting point,  $T_0$  if a repair action is taken (i.e., on all "1" branches). Fatigue reliability patterns for all of the  $2^n$  branches are related to repair realizations for the detail. Figure 1 shows a schematic representation of the fatigue reliability patterns for every branch in a typical event tree when  $n$  equals 2. Note that the "as good as new" assumption may be modified to conditions where either the detail is "not as good as new" or is "better than new" when sufficient data are available for the repair procedure and the altered reliability of the repaired detail. Both the subsequent reliability curve following the repair and the associated costs might in general change for these assumptions relative to the "as good as new" case but such changes are easy to implement.

### 4.3 LIKELIHOOD OF NEEDED REPAIR

The decision whether or not to repair that needs to be made after every inspection of a detail can be interpreted in a probabilistic form. The probability of repair,  $P_R$ , will be employed to describe the decision made after every inspection. This probability may be thought to be the same as the probability of first observation of a crack in the identified detail. An associated limit state function,  $H(\mathbf{X})$ , similar to the one employed for fatigue failure in the AASHTO approach described earlier, may be defined as follows:

$$H(\mathbf{X}) = N_{0.75c} - N = 0.75N_c - N = \frac{0.75A \cdot \Delta}{S_{RE}^3} - N \quad (18)$$

where  $N$  is the number of stress cycles to which the detail is subjected, and  $N_c$  is the critical number of stress cycles to fatigue failure for the detail. Choosing 75 percent of the critical number of stress cycles to correspond to observation of the first crack in fatigue tests was found to be acceptable by Fisher et al (1970). The probability of repair for the detail in question can then be related to an index,  $\gamma$ , and evaluated as:

$$P_R = P(H(\mathbf{X}) \leq 0) = \Phi(-\gamma) \quad (19)$$

Considering the event tree branches, it is found that the probability of repair at every inspection, i.e.  $P_R(T_i)$ , depends on the elapsed time since the last repair. It is assumed that the probabilities of repair at the various inspection times are statistically independent, i.e.,  $P_R(T_i)$  and  $P_R(T_j)$  are statistically



independent for  $i$  not equal to  $j$ . The probability,  $P(B_i)$ , of a branch,  $B_i$ , that includes  $N_R$  repairs can be expressed as the product of  $N_R$  probability of repair terms and  $(N-N_R)$  probability of non-repair terms.

With the help of this event tree approach, and branch probabilities, we can now define the cost of inspections, the cost of repairs, the cost associated with failure for a specified detail. These costs will then be employed in the objective function for the optimization problem.

#### 4.4 COST OF INSPECTIONS

Let  $K_I$  represent the cost of a single inspection of the specified detail. Then, the total cost of inspections over the service life,  $C_I$ , can be represented as:

$$C_I = \sum_{i=1}^n K_I \quad (20)$$

#### 4.5 COST OF REPAIRS

Let  $K_R$  represent the cost of a single repair of the specified detail. Because of the different repair realizations of the detail as given by the event tree, the cost of repair at the time  $T_i$  is the product of  $K_R$  and  $E[R_i]$ , the expected number of repairs at  $T_i$ . Let  $R_i$  denote the repair event at time,  $T_i$  and  $B_j^i$  denote branch  $j$  of the event tree at time,  $T_i$ . The expected number of repairs at  $T_i$  can be expressed as:

$$E[R_i] = \sum_{j=1}^{2^{i-1}} P(R_i \cap B_j^i) \quad (21)$$

The total cost of repairs for the detail over the service life,  $C_R$ , can be represented as:

$$C_R = \sum_{i=1}^n K_R \cdot E[R_i] \quad (22)$$

#### 4.6 COST OF FAILURE

The cost of failure,  $C_F$ , is meant to represent the expected cost resulting from consequences of a failure. If the detail/member under consideration is fracture-critical, its failure could cause failure of the span where the detail is located or even failure of the entire steel bridge. Hence, the cost of failure should include the possible cost of rebuilding a span or the entire bridge, as appropriate, as well as costs due to lost use, injuries, fatalities, etc. – not all of which are easily and uncontroversially estimated. Nevertheless, all of these potential costs associated with a failure are summed to yield a quantity,  $K_F$ . The possibility of the failure consequence is the other term that should be included in the cost of failure. In addition, the scenarios created by the event tree should also be concerned in the evaluation of cost of failure. Let  $F$  denote the event that the detail in question fails and  $B_i$  denote branch  $i$  of the event tree. Then, the expected cost of failure for the specified detail over the service life may be defined as:

$$C_F = \sum_{i=1}^{2^n} \left\{ \frac{1}{T_f - T_0} \int_{T_0}^{T_f} K_F \cdot P(F \cap B_i) dT \right\} \quad (23)$$

Considering all the possible scenarios of the event tree for the detail, the reliability index  $E[\beta]$  can be represented as:

$$E[\beta] = -\Phi^{-1} \left( \sum_{j=1}^{2^n} P(F | B_j) \cdot P(B_j) \right) \quad (24)$$

Substituting Eq. (24) into Eq. (23), the cost of failure may finally be expressed as:

$$C_F = \frac{1}{T_f - T_0} \int_{T_0}^{T_f} K_F \cdot \Phi(-E[\beta]) dT \quad (25)$$

#### 4.7 TOTAL COST

With definitions of the cost of inspections, repairs, and failure for the specified detail, the total cost,  $C_T$ , may be represented as:

$$C_T = C_I + C_R + C_F \quad (26)$$

$$C_T = \left\{ \sum_{i=1}^n K_I \right\} + \left\{ \sum_{i=1}^n K_R \cdot E[R_i] \right\} + \left\{ \frac{1}{T_f - T_0} \int_{T_0}^{T_f} K_F \cdot \Phi(-E[\beta]) dT \right\} \quad (27)$$

#### 4.8 CONSTRAINTS

The number of inspections,  $n$ , and the inspection times,  $T_1 \dots T_n$ , are variables for the optimization problem. One obvious constraint on the inspection times may be expressed as:

$$T_0 < T_1 < K < T_n < T_f \quad (28)$$

Usually, restrictions are placed on the time between inspections such that this inter-inspection interval is neither too large (upper bound,  $T_{\max}$ ) nor too short (lower bound,  $T_{\min}$ ). Such constraints on the inspection interval may be required by local and state transportation agencies. Hence, a second constraint on inspection times for the optimization problem is:

$$T_{\min} \leq T_i - T_{i-1} \leq T_{\max}, \quad i = 1, 2, \dots, n \quad (29)$$

It is also usually required to keep the safety (or reliability) above a certain level. This requirement can be achieved by defining a target reliability index,  $\beta_{\min}$ , which is the minimum acceptable safety tolerance for the specified detail. Thus, a constraint to be included in our optimization problem may be defined as:

$$E[\beta(T_i)] \geq \beta_{\min}, i = 1, 2, \dots (n+1) \quad \text{where } T_{n+1} = T_f \quad (30)$$

#### 4.9 FORMULATION OF THE OPTIMIZATION PROBLEM

In summary, the optimization problem for the inspection scheduling may be formulated as follows:

$$\min_{n, T_1, \dots, T_n} C_T = \left\{ \sum_{i=1}^n K_I \right\} + \left\{ \sum_{i=1}^n K_R \cdot E[R_i] \right\} + \left\{ \frac{1}{T_f - T_0} \int_{T_0}^{T_f} K_F \cdot \Phi(-E[\beta]) dT \right\} \quad (31)$$

$$\text{s.t.} \quad T_0 < T_1 < \mathbf{K} < T_n < T_f$$

$$T_{\min} \leq T_i - T_{i-1} \leq T_{\max}, \quad i = 1, 2, \dots n$$

$$E[\beta(T_i)] \geq \beta_{\min}, \quad i = 1, 2, \dots (n+1)$$

Minimizing the total cost, a set of inspection times,  $T_i$ , may be found. In addition, changing the number of inspections,  $n$ , the total cost corresponding to the different number of inspections may be compared so as to finally yield the optimization solution.

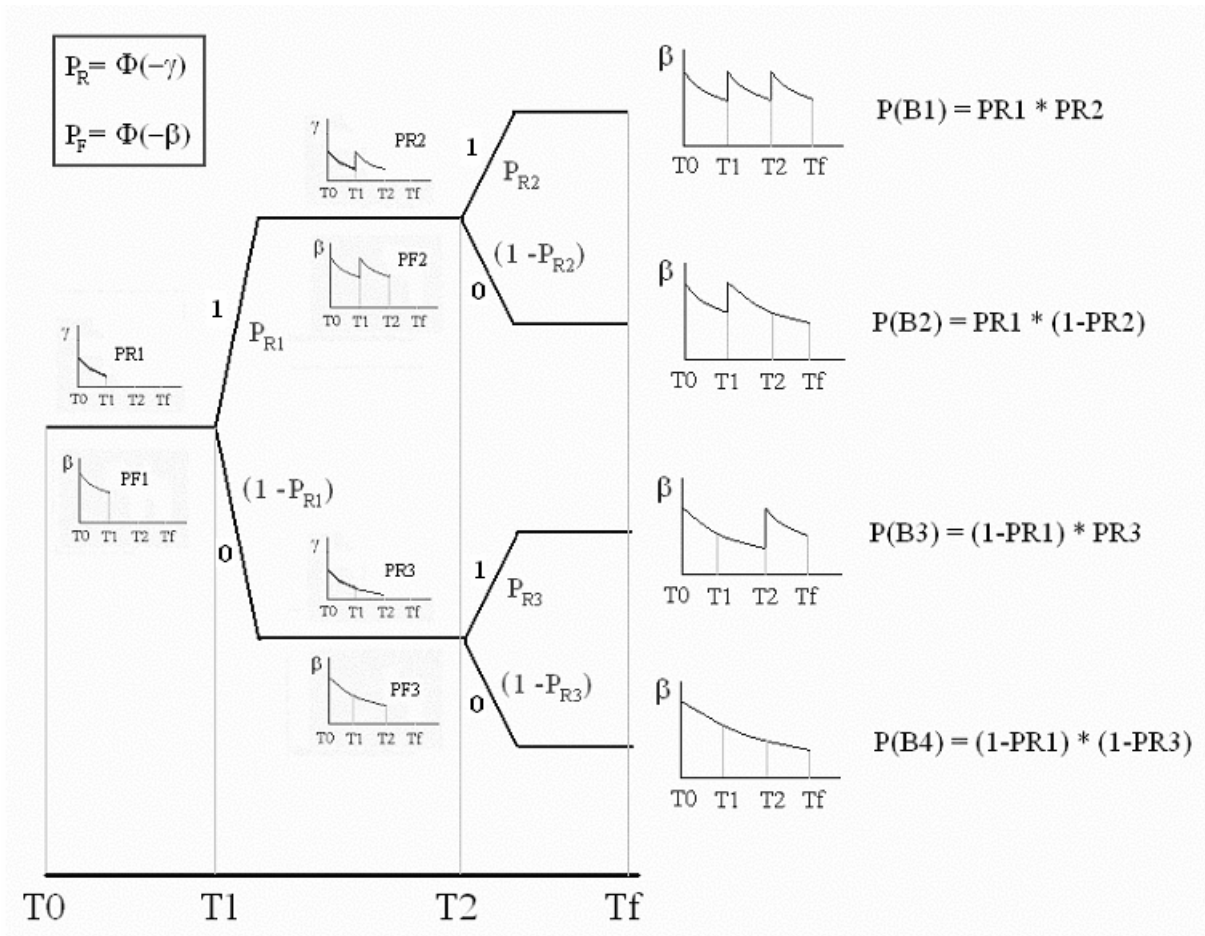


**FIGURE 1** Representative Event Tree showing Inspection and Repair Realizations (similar to one defined by Frangopol et al (1997)).

## CHAPTER 5. NUMERICAL EXAMPLES

### 5.1 PLATE GIRDER BRIDGE EXAMPLE

The example bridge studied here is the 680-ft long Brazos River Bridge in Texas, which was built in 1972. Figure 2 shows the layout of the Bridge as well as a magnified view of the selected fatigue detail, which is classified as a Category E detail as per the AASHTO Specifications. This detail located in the leftmost 150-ft span is analyzed. The stress range parameter,  $S_{R0}$ , applied on this detail is 6.13 ksi as a Rayleigh distribution is assumed for the stress ranges (see Eq. (2)). The target reliability  $\beta_{min}$  for the detail is assumed to be 3.7, corresponding to a failure probability of approximately 1/10000. Additionally,  $T_{min} = 0.5$ yr and  $T_{max} = 2.0$ yr are taken to be constraints on the inter-inspection times. Two sets of relative costs of inspection, repair and failure: (i)  $K_I : K_R : K_F = 1 : 1.3 \times 10^2 : 4 \times 10^5$ ; and (ii)  $K_I : K_R : K_F = 1 : 2.6 \times 10^2 : 4 \times 10^5$  are considered for illustration. The number of stress cycles per truck passage,  $C_s$ , and the Average Daily Truck Traffic, ADTT, are taken to be 1 and 84, respectively (see Eq. (12)). The service life is taken to be 50 years.

After applying the AASHTO fatigue analysis approach, the fatigue reliability,  $\beta$ , of the specified detail over the service life is shown in Fig. 3. The target reliability level,  $\beta_{min}$ , of 3.7 is also shown in the figure. It can be seen that the fatigue reliability of the chosen detail is below the target reliability by the thirteenth year.

First, we will assume that in year 2002 (i.e., 30 years after 1972), no crack was found or that the crack in the detail was repaired to its original condition. To avoid too many inspections and to simultaneously meet the 2-year inspection interval required by the Federal Highway Administration (FHWA), the constraints on inspection intervals,  $T_{min}$  and  $T_{max}$ , are taken to be 0.5 and 2 years, respectively. With an “as good as new” repair policy, and for the relative costs of  $K_I : K_R : K_F = 1 : 1.3 \times 10^2 : 4 \times 10^5$ , it is found in Fig. 4 that the optimal number of inspections for the next twenty years is eleven and the associated optimal inspection schedule is as shown in Fig. 5 where, for comparison, an *ad hoc* periodic inspection schedule is also shown. The optimal inspection times in years are  $\mathbf{T} = (2.0, 4.0, 6.0, 8.0, 10.0, 12.0, 13.5, 14.0, 14.5, 15.0, 15.5) + 30$ . On comparing the optimal inspection schedule with the periodic two-year interval schedule, the total relative cost (162.7) of the optimal schedule is found to be less than the total cost (168.9) of the periodic schedule. Though the optimal schedule requires two more inspections than the periodic schedule, these additional inspections and the short interval between inspections after the bridge reaches 42 years of age reduces the risk of the detail’s failure. This fact can be confirmed by the reduced cost associated with failure in the total cost for the optimal schedule. Therefore, the optimal schedule clearly represents the preferred choice for inspecting this detail over its planned service life.

Upon releasing the constraints on  $T_{max}$ , it is found as shown in Fig. 6 that only five inspections are required to achieve the optimal schedule with an associated total cost of 157.6, which is less than the total cost (162.7) of the previous optimal schedule with  $T_{max} = 2$  yrs. The inspection times in years are  $\mathbf{T} = (13.2, 14.1, 14.6, 15.1, 15.6) + 30$  and note that the reliability index,  $\beta$ , is equal to exactly 3.7 at  $T_I$  (13.2 yrs) and  $T_f$  (20 yrs). No inspections are needed before the reliability curve first hits the target reliability level at 13.2 yrs; also, no inspections are needed after the bridge has completed 45.6 yrs of its planned life. Because of this, the total cost is lower than for the case where the constraint on  $T_{max}$  is included.

For the second case with  $T_{max} = 2$  yrs and the relative costs of  $K_I : K_R : K_F = 1 : 2.6 \times 10^2 : 4 \times 10^5$ , nine inspection times for the next twenty years are needed and the optimal inspection times in years are  $\mathbf{T} = (1.7, 3.4, 5.4, 7.4, 9.4, 11.4, 13.4, 15.1, 17.1) + 30$  as shown in Fig. 7 where again a two-year

periodic inspection interval schedule is also shown. Though the number of inspections (nine) is the same as with the periodic schedule, the total cost (200.5) for the optimal schedule is still lower than the total cost (211.7) for the periodic schedule. After removing the constraint on  $T_{max}$ , again, it is found in Fig. 8 that fewer (four) inspection times,  $\mathbf{T} = (10.8, 13.5, 15.1, 17.1) + 30$ , are needed to reach the optimal schedule with the total cost of 195.0, which, again, is lower than the total cost of 200.5 for the optimal schedule that uses the constraint,  $T_{max} = 2$  yrs.

## 5.2 BOX GIRDER BRIDGE EXAMPLE

We consider a newly built box girder bridge with a center crack in the bottom flange (width = 42 in) as shown in Fig. 9. This example bridge is adapted from one described by Zhao et al. (1994) for which we seek an optimal inspection schedule for the next twenty years.

Two cases of relative costs of inspection, repair and failure: (i)  $K_I : K_R : K_F = 1 : 3 \times 10^2 : 3.6 \times 10^6$ ; and (ii)  $K_I : K_R : K_F = 1 : 6 \times 10^2 : 3.6 \times 10^6$  are considered here. The variables,  $C_s$ ,  $\beta_{min}$ , and ADTT, are taken to be 1, 3.7 and 300 respectively. The random variables related to considerations for a center crack in the bottom flange are listed in Table 2 and the geometry function (see Eq. (17b)) for this crack geometry may be expressed as:

$$Y(a) = \left[ 1 - 0.025(a/b)^2 + 0.06(a/b)^4 \right] \cdot \sqrt{\sec\left(\frac{\pi a}{2b}\right)} \quad (32)$$

Since the detail shown in Fig. 9 is not specifically defined in the AASHTO Specifications, the procedure described for non-AASHTO type details is applied and a fatigue reliability curve from a FORM (First-Order Reliability Method) computation leads to the time-dependent reliability curve shown in Fig. 10. It can be seen that, without intervention or repair of some sort, the fatigue reliability of the chosen detail would fall below the target reliability of 3.7 by the fifteenth year.

For the relative costs of  $K_I : K_R : K_F = 1 : 3 \times 10^2 : 3.6 \times 10^6$ , the reliability curves for optimization schedules in two cases, where  $T_{max} = 2$  yrs as well as where no  $T_{max}$  constraint is imposed, are shown in Fig. 11. It may be seen that, for the optimal schedule constrained by  $T_{max} = 2$  yrs, the optimal number of inspections is ten with a total cost of 322.4 and the inspection times in years,  $\mathbf{T} = (2.0, 4.0, 6.0, 8.0, 10.0, 10.5, 11.0, 11.5, 12.0, 12.5)$ . Not unexpectedly, the optimal schedule without a  $T_{max}$  constraint required fewer (six) inspections and costs less (318); the associated inspection times in years,  $\mathbf{T} = (10.3, 10.8, 11.3, 11.8, 12.3, 12.8)$ . Both optimal schedules result in lower costs than the total cost (396.9) for a two-year periodic inspection schedule that is required by the FHWA.

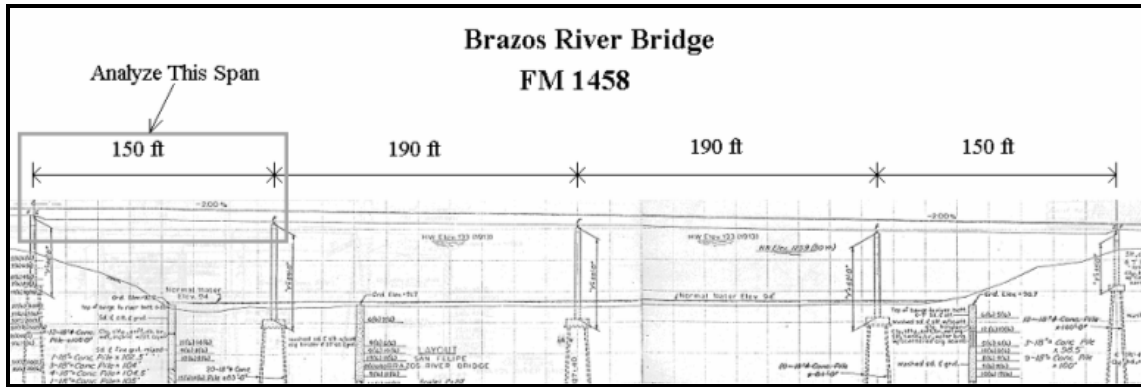
For the second case with higher repair costs, similar findings as in the case with the lower repair costs are noted as shown in Fig. 12. The optimal schedule without a constraint on  $T_{max}$  requires fewer inspections (four) in twenty years and costs less (395.8) than the inspection times (nine) and associated cost (430.1) for the optimal schedule when  $T_{max} = 2$  yrs. The inspection schedules in years for the cases with  $T_{max}$  bounded and unbounded are  $\mathbf{T} = (0.5, 1.0, 1.5, 2.9, 4.9, 6.9, 8.9, 10.9, 12.9)$  and  $\mathbf{T} = (0.5, 1.0, 1.5, 14.6)$ , respectively.

## 5.3 GENERAL CONCLUSIONS

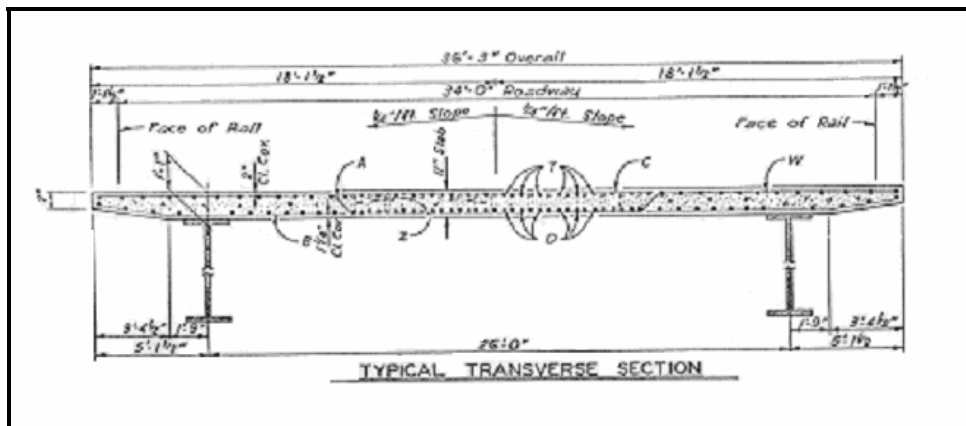
The illustrations presented above demonstrate the application of the optimal inspection scheduling procedure for both, a plate girder bridge and a box girder bridge. Discussions related to the results are presented in Chapter 6.

**Table 5.1. Variables related to Center Crack Growth in the Bottom Flange for the Box Girder Example.**

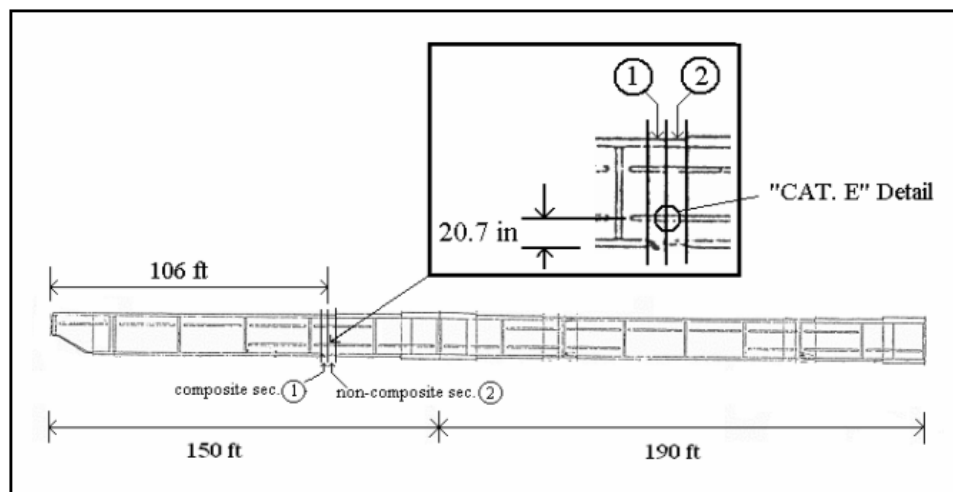
Variable	Type	Mean	COV
$a_0$	lognormal	0.010	0.500
$a_c$	constant	1.000	0.000
$a_R$	constant	0.200	0.000
$C$	lognormal	$2.05 \times 10^{-10}$	0.630
$B$	normal	3.000	0.100
$S_{R0}$	constant	6.334	0.000



(a)



(b)



(c)

**FIGURE 2. Brazos River Bridge showing (a) entire bridge in elevation; (b) a typical transverse section; and (c) a detail of interest for fatigue reliability.**



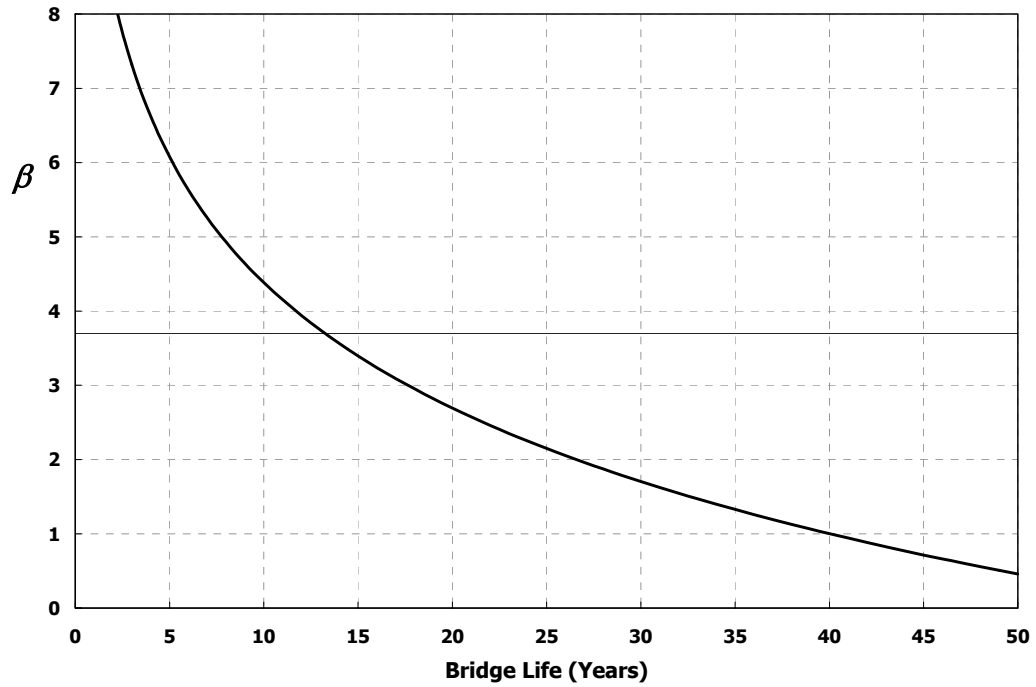


**FIGURE 3. Fatigue Reliability of the Chosen Detail over 50 years for the Plate Girder Numerical Studies.**

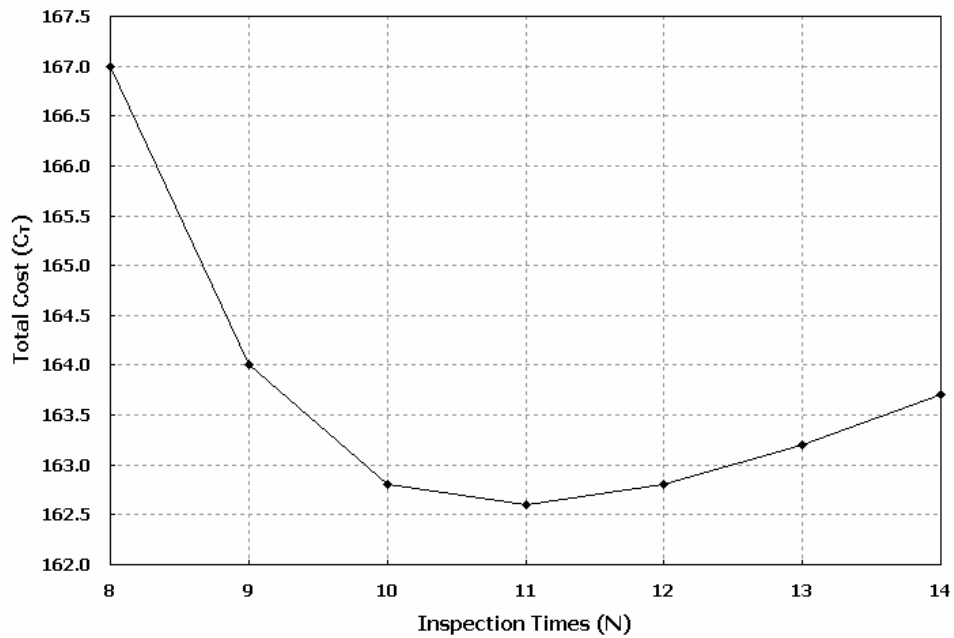


**FIGURE 4. Optimal total cost as a function of the number of inspections for the chosen detail ( $K_I : K_R : K_F = 1 : 1.3 \times 10^2 : 4 \times 10^5$ ).**

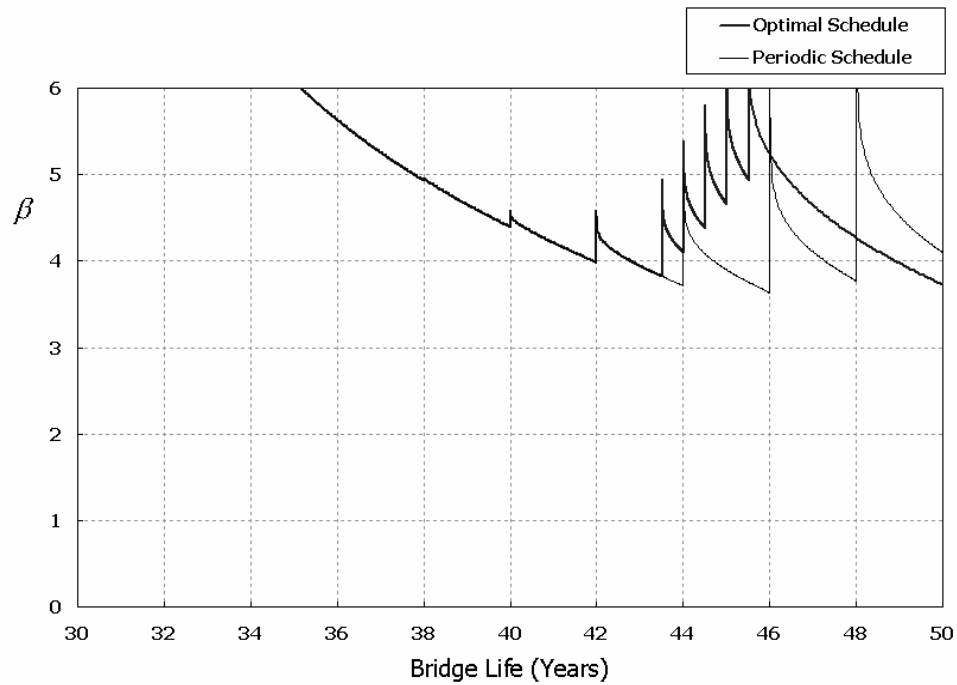


**FIGURE 5. Optimal inspection schedule ( $T_{min} = 0.5$  yrs,  $T_{max} = 2$  yrs) for the case of  $K_I : K_R : K_F = 1 : 1.3 \times 10^2 : 4 \times 10^5$ ,  $C_T = 162.7$ .**

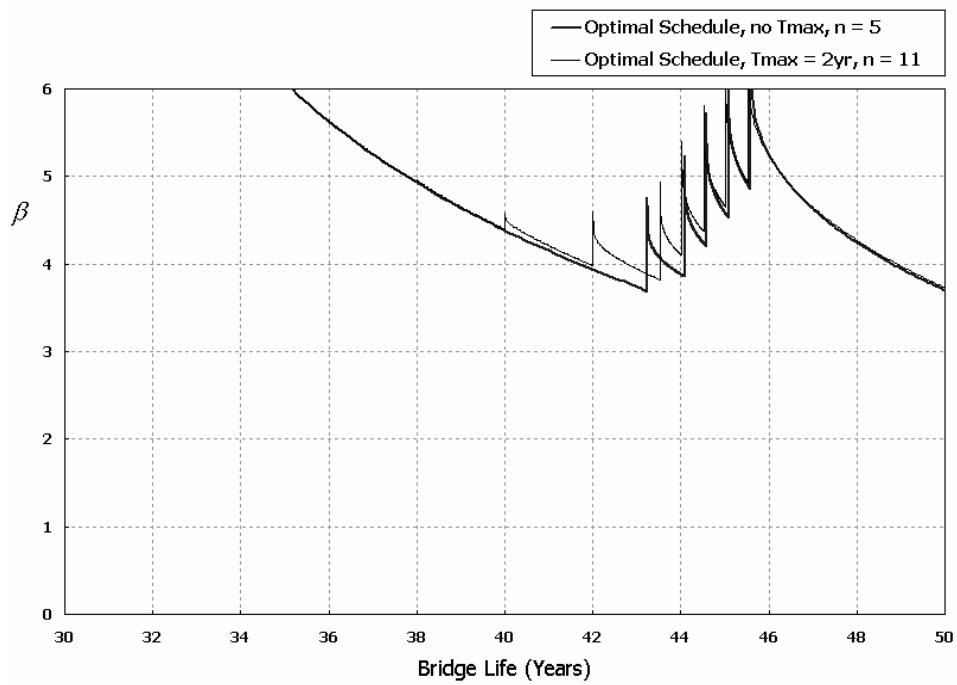


**FIGURE 6. Optimal Inspection Schedule ( $T_{max}$  unbounded) for the case of  $K_I : K_R : K_F = 1 : 1.3 \times 10^2 : 4 \times 10^5$ ,  $C_T = 157.6$ .**

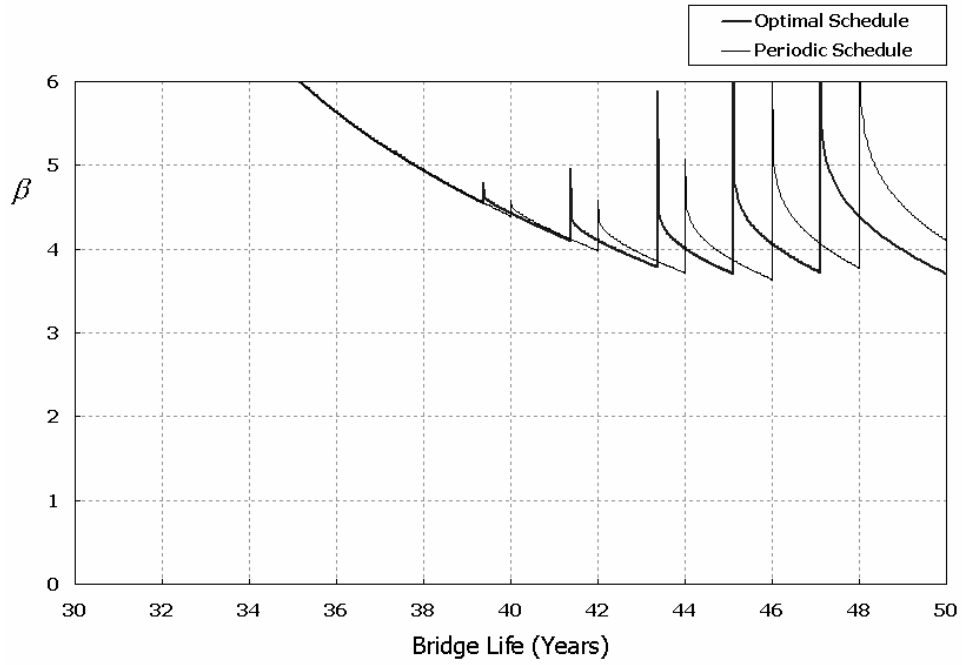


**FIGURE 7. Optimal inspection schedule ( $T_{min} = 0.5$  yrs,  $T_{max} = 2$  yrs) for the case of  $K_I : K_R : K_F = 1 : 2.6 \times 10^2 : 4 \times 10^5$ ,  $C_T = 200.5$ .**

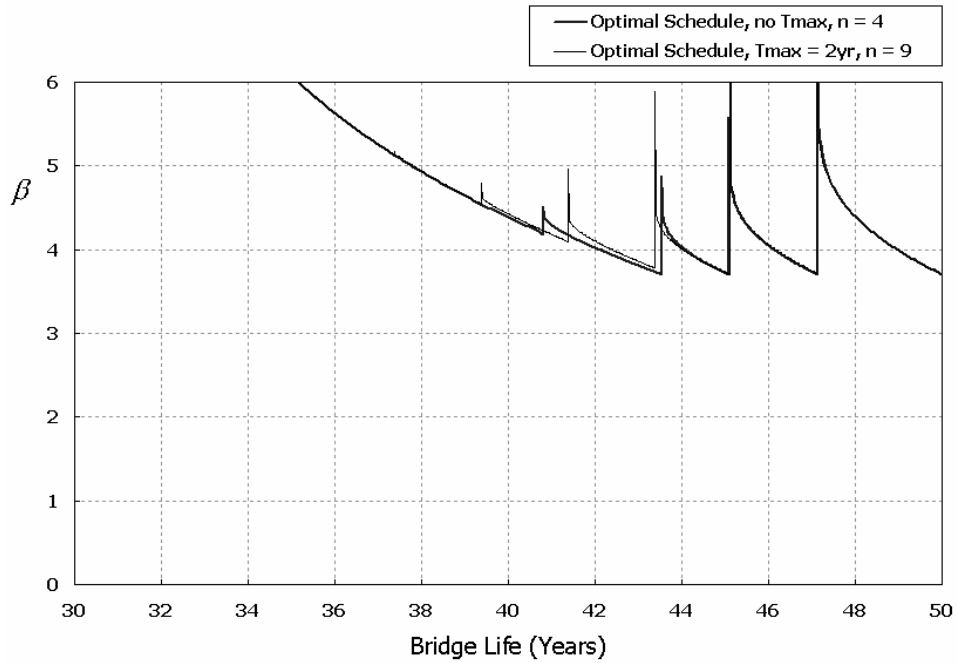


**FIGURE 8. Optimal Inspection Schedule ( $T_{max}$  unbounded) for the case of  $K_I : K_R : K_F = 1 : 2.6 \times 10^2 : 4 \times 10^5$ ,  $C_T = 195.0$ .**

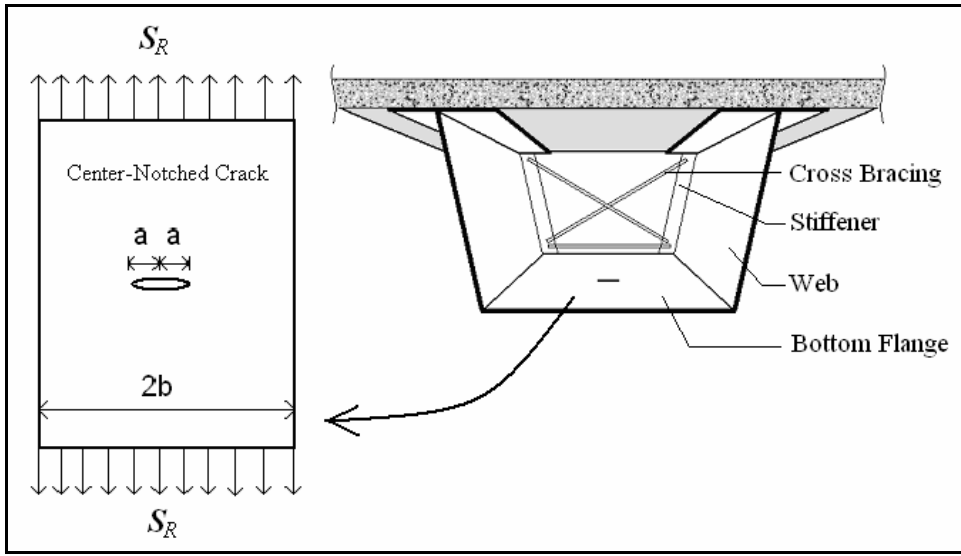


**FIGURE 9. Illustration of the Box Girder Section and Center-Notched Crack in Bottom Flange studied in the Numerical Example.**

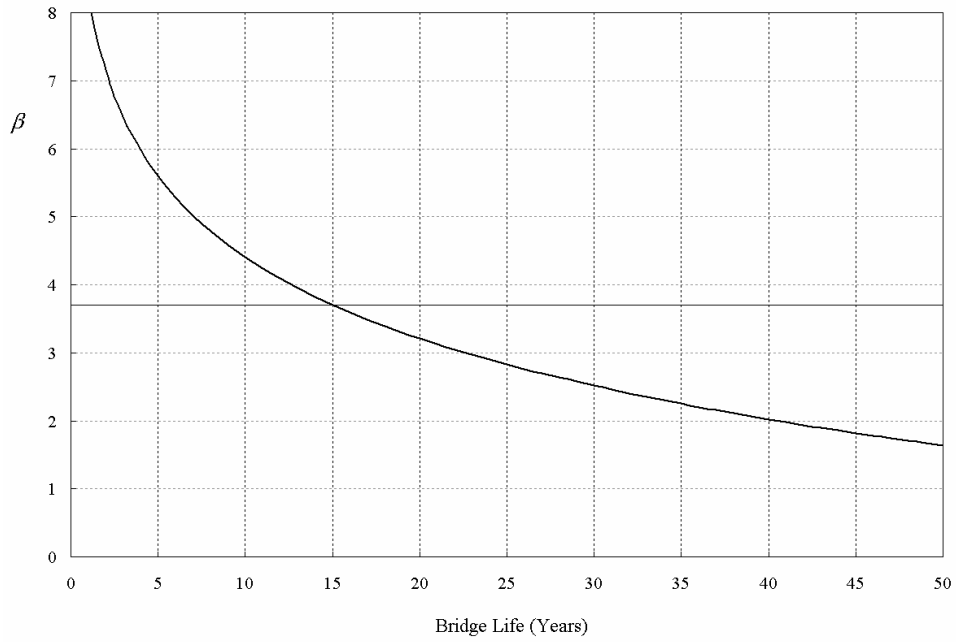


**FIGURE 10. Fatigue Reliability of the Chosen Detail over 50 years for the Box Girder Numerical Studies.**

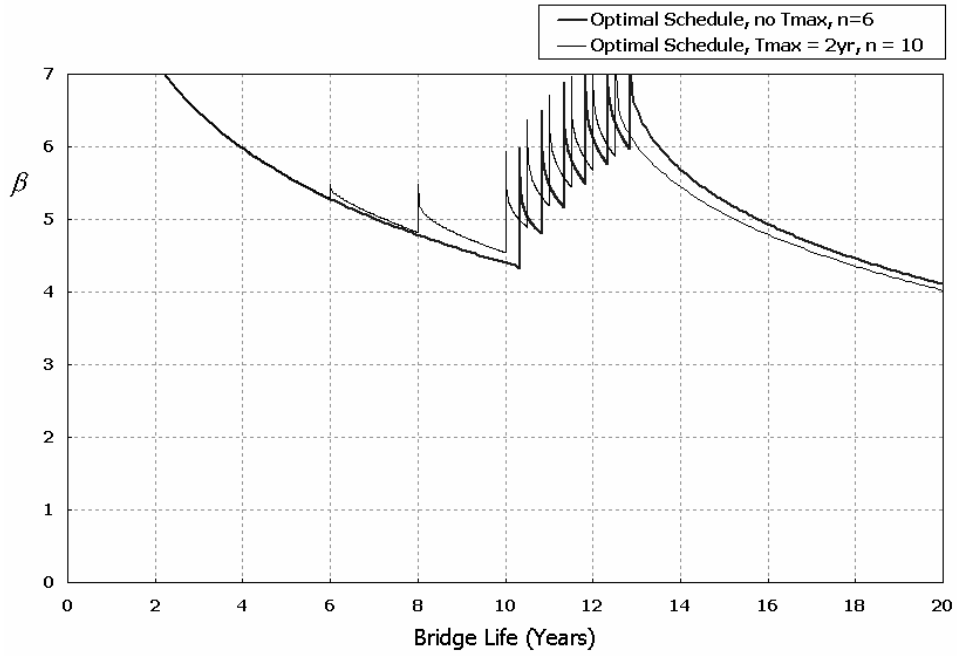


FIGURE 11. Optimal Inspection Schedules with  $T_{max} = 2$  yrs and for unbounded  $T_{max}$  for the Case of  $K_I : K_R : K_F = 1 : 3 \times 10^2 : 3.6 \times 10^6$ .

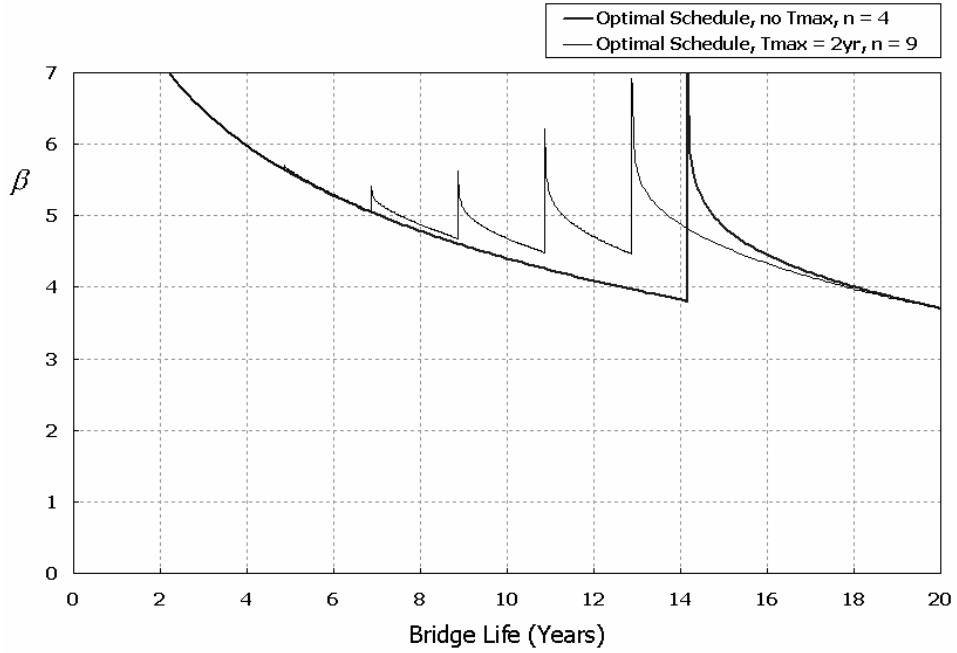


FIGURE 12. Optimal Inspection Schedules with  $T_{max} = 2$  yrs and for unbounded  $T_{max}$  for the Case of  $K_I : K_R : K_F = 1 : 6 \times 10^2 : 3.6 \times 10^6$ .



## CHAPTER 6. DISCUSSION AND CONCLUSIONS

From the results presented, it can be observed that an increase in the number of inspections,  $n$ , tends to increase inspection and repair costs but typically decreases expected failure costs. The optimal result (or lowest cost) occurs for a number,  $n_{opt}$ , of inspections where the decrease in failure costs starts to become smaller than the increase in inspection and repair costs. Comparing the optimal schedules in the two examples studied, the lower relative repair cost cases required more inspections to reach the optimal point while the higher relative repair cost cases required fewer inspections to yield the minimum costs. Clearly, the relative costs of inspection, repair, and failure all affect the optimization results in a very direct manner, regardless of whether or not a constraint on  $T_{max}$  is imposed.

The maximum time between inspections,  $T_{max}$ , is an important constraint that influences the number of inspections, the total cost, and the inspection strategy. When the inspection scheduling is constrained by  $T_{max}$ , a greater number of inspections results which raises the fatigue reliability of the detail and, thus, lowers the expected cost of failure. However, the cost of inspections and repairs increase and the total cost grows as a result. When the constraint on  $T_{max}$  is removed, the repair strategy changes so as to require inspections only when the reliability curve gets close to the target reliability; this results in lower total costs.

It is seen that a periodic two-year inspection schedule over the planned service life as is required by the FHWA for steel bridges will not be the optimal schedule for some details if one is interested in keeping costs low as well as maintaining safety. Though this periodic schedule keeps the fatigue reliability at a higher level than the optimal schedules obtained for the example bridge studied here, a larger number of inspections and repairs over the service life cause an increase in total cost. The reliability-based fatigue inspection strategy presented here yields the optimal inspection schedule maintaining prescribed safety levels for lower costs. The optimization results are affected by the time-dependent fatigue reliability of the detail in question, the imposed constraints (i.e., on the minimum acceptable reliability and on the inspection interval), and the relative costs of inspection, repair and failure. The influences of the constraints on the interval between inspections (at least on the upper bound of this interval), and of the relative costs of inspection, repair and failure were highlighted in the numerical examples presented.

Reliability-based inspection scheduling offers a rational method to arrive at inspection and maintenance strategies for steel bridges. Applying the procedure described for various types of details, bridge authorities can optimally allocate their maintenance budgets in an efficient manner without compromising the safety of their bridges. This optimal scheduling procedure may also be applied to other degrading civil infrastructure systems if the reliability, costs, and the related random variables affecting performance can be quantified.





## REFERENCES

- (1) AASHTO, American Association of State Highway and Transportation Officials, AASHTO LRFD Bridge Design Specifications, Customary U.S. Units, 2<sup>nd</sup> ed., Washington, D.C., 1998.
- (2) Fisher, J. W., Frank, K. H., Hirt, M. A and McNamee, B. M., Effect of Weldments on the Fatigue Strength of Steel Beams, National Cooperative Highway Research Program Report 102, 1970.
- (3) Frangopol, D. M., Lin, K. Y. and Estes, A., Life-Cycle Cost Design of Deteriorating Structures, Journal of Structural Engineering, ASCE, Vol. 123, No. 10, 1997, pp.1390-1401.
- (4) Keating, P. B. and Fisher, J. W., Review of Fatigue Tests and Design Criteria on Welded Details, Fritz Engineering Laboratory Report 488-1(85), Lehigh University, Bethlehem, PA, Oct. 1985.
- (5) Madsen, H. O., Krenk, S. and Lind, N. C., 1985. Methods of Structural Safety, Prentice-Hall Inc., N.J.
- (6) Madsen, H. O., Optimal Inspection Planning for Fatigue Damage of Offshore Structures, 5th International Conference on Structural Safety and Reliability, 1989, pp. 2099-2106.
- (7) Miner, M. A., Cumulative Damage in Fatigue, J. Appl. Mech., Vol. 12, No. 3, 1945, A-159-A-164.
- (8) Moses, F., Schilling, C. G. and Raju, K. S., Fatigue Evaluation Procedures for Steel Bridges, National Cooperative Highway Research Program Report 299, 1987.
- (9) Schilling, C. G., Lateral-Distribution Factors for Fatigue Design, Journal of the Structural Division, Proceedings of ASCE, Vol. 108, No. ST9, September, 1982, pp. 2015-2033.
- (10) Schilling, C. G., Impact Factors for Fatigue Design, Journal of the Structural Division, Proceedings of ASCE, Vol. 108, No. ST9, September, 1982, pp. 2034-2044.
- (11) Schilling, C. G., Klippstein, K. H., Barsom, J. M., and Blake G. T. Fatigue of Welded Steel Bridge Members under Variable-Amplitude Loadings, National Cooperative Highway Research Program Report 188, 1978.
- (12) Snyder, R. E., Likins, G. E. and Moses, F., Loading Spectrum Experienced by Bridge Structures in the United States, Report FHWA/RD-85/012, Bridge Weighing Systems, Inc., Warrensville, OH, Feb. 1985.
- (13) Sommer, A. M., Nowak, A. S. and Thoft-Christensen, P., Probability-Based Bridge Inspection Strategy, Journal of Structure Engineering, ASCE, Vol. 119, No. 12, December, 1993, pp. 3520-3536.

- (14) Sorensen, J. D., Faber, M. H., Rackwitz, R. and Thoft-Christensen, P., Modelling in Optimal Inspection and Repair, OMAE, Vol. 2, Safety and Reliability, 1991, pp. 281-288.
- (15) Thoft-Christensen, P. and Sorensen, J. D., Optimal Strategy for Inspection and Repair of Structural Systems, Civil Engineering Systems, Vol. 4, June, 1987, pp. 94-100.
- (16) Wirsching, P. H. and Chen, Y. N., Consideration of Probability Based Fatigue Design for Marine Structures, Marine Structure, 1, 1988, pp. 23-45.
- (17) Zhao, Z., Haldar, A. and Breen, F. L., Fatigue-Reliability Evaluation of Steel Bridges, Journal of Structural Engineering, ASCE, Vol. 120, No. 5, May 1994, pp. 1608-1623.